Research Article Vol. 2, No. 10 / 15 Oct 2023 / Optics Continuum 2178
OPTICS CONTINUUM

Enhancement of Er luminescence from bridge-type photonic crystal nanocavities with Er, O-co-doped GaAs

ZHIDONG FANG,[1] JUN TATEBAYASHI,[1,2,*] RYOHEI HOMI,[1] MASAYUKI OGAWA,[1] HIROTAKE KAJII,[3] MASAHIKO KONDOW,[3] KYOKO KITAMURA,[1,4] BRANDON MITCHELL,[3,5] SHUHEI ICHIKAWA,[1,3] AND YASUFUMI FUJIWARA[1]

[1]*Division of Materials and Manufacturing Science, Graduate School of Engineering, Osaka University, 2-1 Yamadaoka, Suita, Osaka 565-0871, Japan*
[2]*Center for Quantum Information and Quantum Biology, Osaka University, 2-1 Yamadaoka, Suita, Osaka 565-0871, Japan*
[3]*Division of Electrical, Electronic and Infocommunications Engineering, Graduate School of Engineering, Osaka University, 2-1 Yamadaoka, Suita, Osaka 565-0871, Japan*
[4]*Department of Electronics, Kyoto Institute of Technology, Matsugasaki, Sakyo-ku, Kyoto 606-8585, Japan*
[5]*Department of Physics and Engineering, West Chester University, West Chester, PA 19383, USA*
[*]*tatebaya@mat.eng.osaka-u.ac.jp*

Abstract: A bridge-type photonic crystal (PhC) nanocavity based on Er,O-codoped GaAs is employed to realize enhancement of Er luminescence. By adjusting the structural design and measurement temperature, the cavity mode's wavelength can be coupled to Er luminescence. The peak emission intensity from an Er-2O defect center was enhanced 7.3 times at 40 nW pump power and 77 K. The experimental Q-factor is estimated to be over 1.2×10^4, and the luminescence intensity shows superlinearity with excitation power, suggesting Er luminescence amplification. This result would pave the way towards the realization of highly efficient single-photon emitters based on rare-earth elements.

1. Introduction

Rare-earth ions (REIs), particularly trivalent erbium (Er^{3+}), have attracted much interest in quantum information science, serving as ensemble-based memories and single-photon emitters (SPEs) [1,2]. Atomic-like defects, well-defined optically addressable spins, long coherence times, narrow emission lines, and weak coupling to phonons, make them ideal for quantum computing, cryptography, memory, and communication applications [3–10]. The emerging field of nanophotonics and advancements in nanofabrication techniques have further highlighted the potential of REIs in creating efficient optical devices for quantum information applications, including quantum key distribution and optical quantum computation [11–13]. Above all, SPEs based on REIs doped semiconductors have recently attracted more and more attention due to their narrow, highly coherent transitions [14–17]. However, there is a need for material systems that can function as spin-photon interfaces at room temperature and can be electrically and optically excited [18]. This is because most of the host systems which have been demonstrated for REIs have been complex oxides and other insulators, and hence there would be a huge advantage if SPEs could be realized on compound semiconductors in terms of their compatibility with existing, well-established compound semiconductor-based quantum information devices.

Er^{3+} ions co-doped with oxygen in GaAs form specific luminescent centers, referred to as Er-2O centers, which exhibit sharp luminescence peaks with ultra-high wavelength stability

#501666 https://doi.org/10.1364/OPTCON.501666
Journal © 2023 Received 27 Jul 2023; revised 15 Sep 2023; accepted 18 Sep 2023; published 3 Oct 2023

OPTICS CONTINUUM

against temperature at ~1.54 μm due to intra-*4f*-shell transitions ($^4I_{13/2} \rightarrow {}^4I_{15/2}$) in the telecommunication band [6,7,19–25]. In general, REIs are characterized by partially filled *4f* shells, which are localized inside completely filled *5s* and *5p* shells. This screening of electrons in the *4f* shells results in luminescence with an ultra-high temperature-insensitivity, which has never been attained by the conventional SPEs based on quantum dot systems characterized by their light emission via band-to-band transition process [6,7,19,26]. Our group has so far established the growth of Er, O-co-doped GaAs (GaAs:Er,O) emitting at the telecommunication wavelength of 1.54 μm and demonstrated light-emitting-diodes based on GaAs:Er,O operating at room temperature which would be applicable for electrically injected SPEs [24,27,28]. Recently, our group has been pursuing to couple such Er luminescence with nanocavities including photonic crystals (PhCs) or microdisks (MDs). This is because optical nanocavities with a high quality (Q)-factor and small modal volume can overcome the long lifetime of Er^{3+} luminescence by controlling the emission rate via the Purcell effect [6,12,29–34]. Our group has already realized GaAs:Er,O microdisk resonators and L3-type 2-D PhC nanocavities, which exhibited Q-factors of >9,000 and >5,000, respectively [35,36]. In addition, we have also obtained enhanced Eu luminescence in Eu-doped GaN using PhCs or MDs structures, which would demonstrate the feasibility of using high Q-factor structures to enhance the luminescence of REIs with the highest Q-factor over 10^4 [37–40]. However, further increase of the Q-factor is required to further enhance the luminescence rate of Er, and to eventually achieve the high-efficiency and stable SPEs based on GaAs:Er.O.

In this contribution, we employ a bridge-type 1-D PhC cavity to simplify the structure, further increase the Q-factor, reduce the mode volume, and enhance Er-related luminescence [41,42]. Numerical simulations of the PhC nanobeam cavities are carried out using the finite-difference time-domain (FDTD) method to investigate the fundamental mode and higher-order modes from the cavity emission. In addition, bridge-type PhC cavities with GaAs:Er,O as active components are prepared, and optically characterized at both room and low temperature. The wavelength of the cavity mode is coupled to the Er luminescence by adjusting the structural design and measurement temperature. With a Q-factor of more than 12,000, a 7.3-fold enhancement of Er luminescence is realized.

2. Experimental details

In this work, bridge-type PhC nanocavities based on GaAs:Er,O were fabricated. To tune the cavity mode to couple to Er luminescence, a strategy of scanning every 1 nm for the crystal constant (a) when fabricating the pattern was used. Since there is an air-gap underneath the bridge-type PhCs, a sacrificial layer was used under the active layer. First, epitaxial layers of GaAs:Er,O were grown on GaAs(~20 nm)/AlGaAs(~1μm)/(001) semi-insulating GaAs substrates by low-pressure organometallic vapor phase epitaxy at 76 Torr with triethylgallium and tertiarybutylarsine as group III and V sources and tris(isopropylcyclopentadienyl)erbium Er(i-PrCp)$_3$ for Er doping, as shown in our previous publication [36]. A schematic of the sample structure is illustrated in Fig. 1(a). The thickness of GaAs:Er,O was adjusted to ~250 nm to suppress the generation of multi-modes in the vertical direction. This was achieved by wet etching using 1 mol/L citric acid and 3% concentration of hydrogen peroxide water in a 50:3 mixture to precisely control the thickness of the active layer. Afterward, a periodic lattice consisting of circular holes was formed using electron beam lithography. A mask of the nanocavity design was transferred to the GaAs:Er,O active layer by employing an inductively coupled plasma using 18 sccm of Cl_2 and 12 sccm of BCl_3 as reaction gases and 3 sccm of CH_4 as protective gas. Chlorine was the main etching agent. BCl_3 can remove aluminum oxide and thus achieve deeper and faster etching of AlGaAs. CH_4 can passivate sidewalls by forming a polymer with the etching products [43–45]. Finally, the AlGaAs sacrificial layers were selectively removed by wet etching using hydrofluoric acid, resulting in hollow bridge-type PhC nanocavities.

OPTICS CONTINUUM

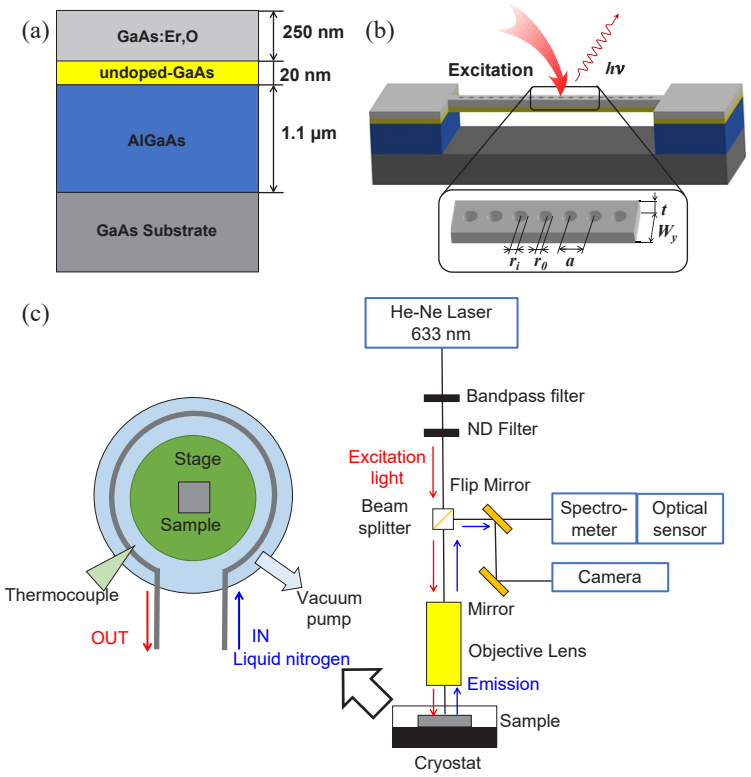

Fig. 1. (a) Schematic diagram of the GaAs:Er,O sample structure. (b) Schematic diagram of a bridge-type PhC. The excitation laser is focused on the center of the bridge-type PhC, and the generated photoluminescence is emitted from the structure. (c) Schematic diagram of the micro-photoluminescence (μ-PL) measurement setup.

In the nanocavity design, the radius of the central hole (r_0) was set to 0.3 times a, i.e., r_0= 0.3a. Then, starting from the central hole and moving outward, the hole diameters were gradually reduced, with the radius of the i^{th} hole (r_i) being set to $r_i = r_0(1\text{-}(i/30)^2)$ nm. A schematic diagram of the bridge-type PhC is shown in Fig. 1(b). Structural characterization of the prepared samples was carried out using scanning electron microscopy (SEM). The luminescence properties of the samples were characterized by micro-photoluminescence (μ-PL) measurements. In the μ-PL measurements, a continuous-wave He-Ne laser (633 nm) was focused on the center of the bridge-type PhC structures to excite the Er-2O luminescence center. The resulting emission was collected by an objective lens with a numerical aperture of 0.42 located above the sample, dispersed with a 0.75 m monochromator, and finally detected using a liquid-nitrogen-cooled InGaAs photodiode array. The sample was mounted on a cryostat, which is equipped with a heater and a tube around the stage to circulate liquid nitrogen, which allows for measurements to be carried out above room temperature and down to ~77 K. For the low-temperature measurements, a vacuum must be created between the pipes and the stage using a rotary pump, which insulates the pipes and prevents the formation of frost. Figure 1(c) shows the schematic diagram of the μ-PL measurement setup.

OPTICS CONTINUUM

3. Results and discussion

In order to explore and optimize the parameters of our bridge-type PhC nanocavities, finite-difference time-domain (FDTD) simulations utilizing commercially available Ansys Lumerical FDTD software were performed. In these simulations, the nanobeam width (W_y) was set to 1.325a. Considering the primary emission wavelength from the Er-2O luminescence center (1538 nm) and the refractive index of GaAs (3.3), the thickness (t) of the bridge-type PhC was set to 278 nm. An electric dipole was placed at the center of the bridge structure as the excitation source in the FDTD simulations since this is where the excitation laser is focused in the experiments. Figure 2(a) shows the simulated spectrum from bridge-type PhC cavity structure with the optimized parameters determined above. In the spectrum, the fundamental mode can be observed along with four additional higher-order modes. The cavity modes can be confirmed by the electric field intensity distribution of the respective modes, as shown in Figs. 2(b) and (c). The simulated mode volume is ~0.8 $(\lambda/n)^3$ for the fundamental mode.

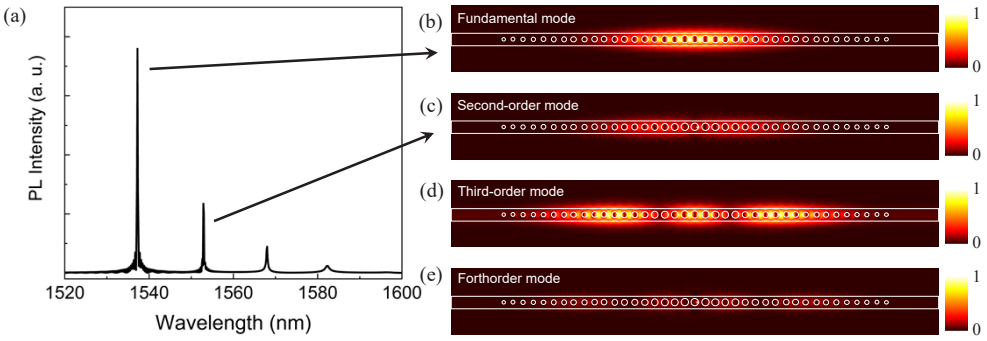

Fig. 2. (a) The simulated spectrum for a bridge-type PhC cavity with 37 holes and a lattice constant of $a = 374$ nm. (b,c,d,e) Calculated distributions of the electric field intensity for (b) fundamental mode,(c) second-order mode, (d) third-order mode and (e) forth-order mode.

Based on the simulation which is stated above, several bridge-type PhC cavities with different a are fabricated, in order to couple the cavity mode to the Er luminescence. SEM images of the typical bridge-type PhC cavity are shown in Figs. 3(a) and (b). In Fig. 3(a), a shadow can be observed under the structure, which confirms the air-gap underneath the structure. The circular holes exhibit good roundness, and it is confirmed that the radii of the holes smoothly decrease from the center hole outward. The lattice constant of the structure in Fig. 3(a) is designed to be 370 nm. Furthermore, the radius of the central hole is 114 nm, which corresponds to the design value of 111 nm with an error of 3 nm. These fabrications errors will result in deviations between the experimental resonant wavelengths and Q-factors and the design values; however, no major structural defects that would inhibit the overall functionality of the cavity were observed.

μ-PL measurements were performed on the sample with a designed lattice constant of $a = 374$ nm at room temperature. The excitation power was 100 μW, and the integration time was 60 s. In Fig. 4(a), two cavity peaks can be observed in the spectrum of the bridge-type PhC within the range of 1520 nm to 1560 nm. Despite the cavity modes not being in resonance with the Er emission, all Er-related emission peaks from the bridge-type PhC sample are enhanced at room temperature as compared to the bulk sample. The increase in all emission peaks at room temperature is a result of the increase in surface area caused by the structure, and thus an increase in the light extraction efficiency. To calculate the resonator Q-factor at room temperature, the spectra were fitted using a Lorentz function. The full width at half maximum (FWHM) of the resonance peak at 1539.6 nm was determined to be 0.13 nm. From this value, the resonator Q-factor of 1.2×10^4 was obtained. However, since the wavelength resolution of the μ-PL setup

OPTICS CONTINUUM

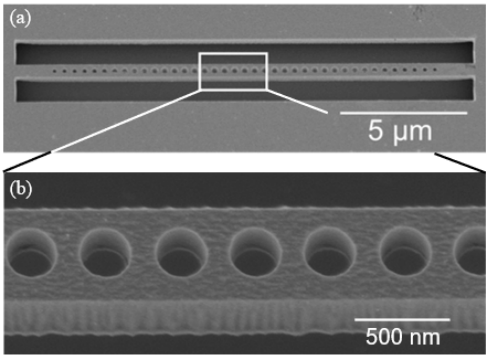

Fig. 3. (a), (b) SEM images of the fabricated bridge-type PhC. (a) SEM image of the overall bridge-type PhC. (b) Local details of the bridge-type PhC. The structure was fabricated with air-gap formed underneath and fabrication errors were effectively controlled.

used in this research is ~0.12 nm, and the FWHM described above is close to this resolution, the actual FWHM may be smaller than 0.12 nm. Thus, the Q-factor of this structure is considered to be more than 1.2×10^4. In addition, it is noted that the relative intensity difference between the first- and second-order modes in the experimental results is different from that in the simulation, which is likely due to the fabrication error [46].

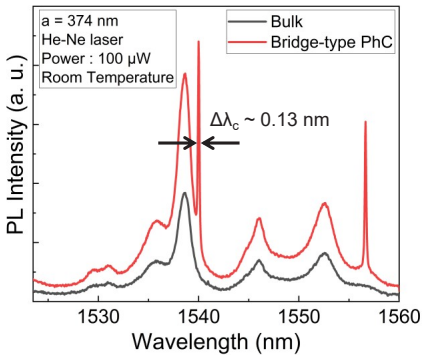

Fig. 4. The μ-PL spectra at room temperature, lattice constant of 374 nm (designed value), and excitation power of 100 μW for bulk (black) and cavity mode (red). All luminescence peaks were enhanced and a Q-factor of more than 1.2×10^4 was obtained at 1539.6 nm.

In order to couple the cavity mode to Er luminescence, we tune the wavelength corresponding to the cavity mode by fabricating different PhCs with different lattice constant a in the same fabrication run and adjusting the temperature for measurements. The emission spectra of the bridge-type PhC nanocavity sample and a bulk sample are shown in Fig. 5(a). The μ-PL spectrum of the bulk material shows the typical emission from the Er-2O center at 1538 nm, while that of the PhC nanocavity shows two sharp, intense peaks originating from the fundamental mode and a higher-order mode of the bridge-type PhC cavity. The designed value for lattice constant of the cavity decreased from 374 nm to 371 nm at 77 K, which blue-shifted the fundamental mode of the bridge-type PhC cavity to be in resonance with the primary emission peak of the Er-2O center. The emission intensity of this peak is enhanced 7.3-fold at a pump power of 40 nW. The linewidth of the fundamental cavity mode is also about 0.13 nm by being fitted using Lorentz function. Therefore, the experimental Q-factor is also estimated to be larger than 1.2×10^4.

OPTICS CONTINUUM

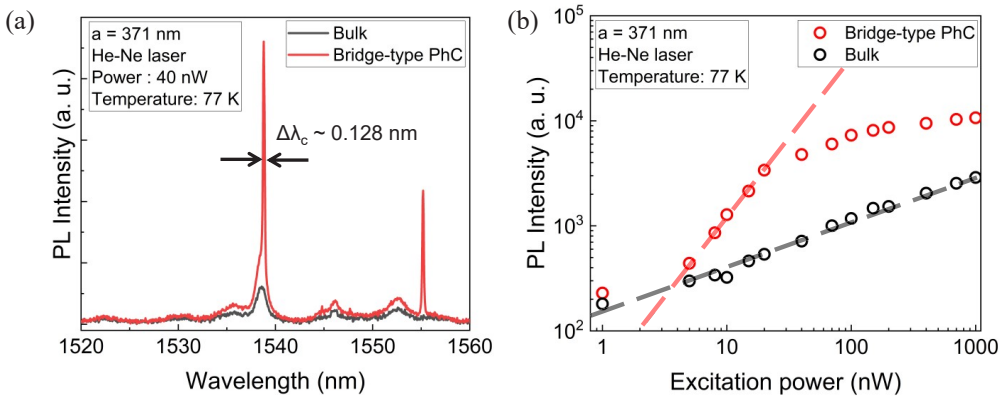

Fig. 5. (a) The μ-PL spectra at 77 K, the lattice constant of 371 nm, and excitation power of 40 nW for bulk (black) and cavity mode (red). The Er luminescence at 1538 nm was enhanced by a factor of 7.3 with a Q-factor of more than 1.2×10^4. (b) The PL intensity of emission from cavity mode (red) and bulk (black) at different excitation powers with lattice constant of 371.25 nm and temperature of 77 K. The superlinearity of the Er luminescence on the excitation power resulting from bridge-type PhC was observed.

Since the linewidth of the emission was already determined to be within the resolution of our detection system, we would like to analyze the reason for the enhancement. We measured the excitation intensity dependence of the bridge-type PhC nanocavity emission to confirm if a nonlinear increase was observed. Peak intensities were determined from the PL spectra of bulk and nanocavity samples at various excitation densities. Figure 5(b) shows a logarithmic plot of the peak intensity of the 1538 nm cavity peaks from the bulk and nanocavity samples. The slope of the curve is superlinear in the range of 5-20 nW, having an exponent of greater than 1, while that of the bulk is nearly linear. After an excitation power of ~100 nW, the slope flattens, which is likely due to the saturation of the Er-2O centers. We observed a superlinear behavior that is similar to our previous result on Er ions in GaAs with MDs [35]. The reason for such a superlinear behavior is likely to be the amplification of Er luminescence emission.

4. Conclusion

In conclusion, we have completed the fabrication of a bridge-type PhC cavity using Er,O co-doped GaAs as the active layer and quantitatively analyzed its characteristics. When the cavity mode is detuned with Er emission, all Er emission peaks are enhanced. The cavity mode can be coupled with Er luminescence by controlling the lattice constant a and the temperature. When the cavity is resonant with Er luminescence, an enhancement of up to 7.3 times occurs at the fundamental mode. In the luminescence spectrum, cavity mode yields an emission linewidth of ~0.13 nm, which is close to the resolution limit of our experimental setup, suggesting an estimated experimental Q-factor exceeding 1.2×10^4. Furthermore, the luminescence intensity of bridge-type PhCs exhibits superlinearity in relation to excitation power, potentially indicating amplification of Er luminescence. This analysis of the enhancement of the optical properties of rare-earth luminescence centers may contribute to the application of Er-2O centers as SPEs for quantum information technology.

Funding. Japan Society for the Promotion of Science (18H05212, 23H00185, 23H05449).

Acknowledgment. This work was partly supported by JST SPRING (Grant No. JPMJSP2138) and the Canon Foundation.

Disclosures. The authors declare that there are no conflicts of interest related to this article.

OPTICS CONTINUUM

Data availability. Data underlying the results presented in this paper are not publicly available at this time but may be obtained from the authors upon reasonable request.

References

1. N. Ohlsson, R. K. Mohan, and S. Kröll, "Quantum computer hardware based on rare-earth-ion-doped inorganic crystals," Opt. Commun. **201**(1-3), 71–77 (2002).
2. C. W. Thiel, T. Böttger, and R. Cone, "Rare-earth-doped materials for applications in quantum information storage and signal processing," J. Lumin. **131**(3), 353–361 (2011).
3. T. Watson, S. Philips, and E. Kawakami, *et al.*, "A programmable two-qubit quantum processor in silicon," Nature **555**(7698), 633–637 (2018).
4. J. J. Morton, A. M. Tyryshkin, and R. M. Brown, *et al.*, "Solid-state quantum memory using the 31P nuclear spin," Nature **455**(7216), 1085–1088 (2008).
5. D. D. Awschalom, L. C. Bassett, and A. S. Dzurak, *et al.*, "Quantum spintronics: engineering and manipulating atom-like spins in semiconductors," Science **339**(6124), 1174–1179 (2013).
6. H. Mäntynen, N. Anttu, and Z. Sun, *et al.*, "Single-photon sources with quantum dots in III–V nanowires," Nanophotonics **8**(5), 747–769 (2019).
7. Ł Dusanowski, D. Köck, and E. Shin, *et al.*, "Purcell-enhanced and indistinguishable single-photon generation from quantum dots coupled to on-chip integrated ring resonators," Nano Lett. **20**(9), 6357–6363 (2020).
8. B. Mitchell, H. Austin, and D. Timmerman, *et al.*, "Temporally modulated energy shuffling in highly interconnected nanosystems," Nanophotonics **10**(2), 851–876 (2020).
9. B. Casabone, C. Deshmukh, and S. Liu, *et al.*, "Dynamic control of Purcell enhanced emission of erbium ions in nanoparticles," Nat. Commun. **12**(1), 3570–3577 (2021).
10. M. Raha, S. Chen, and C. M. Phenicie, *et al.*, "Optical quantum nondemolition measurement of a single rare earth ion qubit," Nat. Commun. **11**(1), 1605–1606 (2020).
11. K. Takemoto, Y. Nambu, and T. Miyazawa, *et al.*, "Quantum key distribution over 120 km using ultrahigh purity single-photon source and superconducting single-photon detectors," Sci. Rep. **5**(1), 14383–14387 (2015).
12. T. Northup and R. Blatt, "Quantum information transfer using photons," Nat. Photonics **8**(5), 356–363 (2014).
13. E. Knill, R. Laflamme, and G. J. Milburn, "A scheme for efficient quantum computation with linear optics," Nature **409**(6816), 46–52 (2001).
14. L. Yang, S. Wang, and M. Shen, *et al.*, "Controlling single rare earth ion emission in an electro-optical nanocavity," Nat. Commun. **14**(1), 1718 (2023).
15. T. Boettger, Y. Sun, and C. Thiel, *et al.*, *Material optimization of Er^{3+}:Y^2SiO^5 at 1.5 um for optical processing, memory, and laser frequency stabilization applications* (SPIE, 2003).
16. D. Serrano, J. Karlsson, and A. Fossati, *et al.*, "All-optical control of long-lived nuclear spins in rare-earth doped nanoparticles," Nat. Commun. **9**(1), 2127 (2018).
17. J.-Y. Huang, P.-J. Liang, and L. Zheng, *et al.*, "Stark tuning of telecom single-photon emitters based on a single Er^{3+}," Chin. Phys. Lett. **40**(7), 070301 (2023).
18. M. E. Reimer and C. Cher, "The quest for a perfect single-photon source," Nat. Photonics **13**(11), 734–736 (2019).
19. S. Hepp, F. Hornung, and S. Bauer, *et al.*, "Purcell-enhanced single-photon emission from a strain-tunable quantum dot in a cavity-waveguide device," Appl. Phys. Lett. **117**(25), 254002 (2020).
20. K. Takahei and A. Taguchi, "Selective formation of an efficient Er-O luminescence center in GaAs by metalorganic chemical vapor deposition under an atmosphere containing oxygen," J. Appl. Phys. **74**(3), 1979–1982 (1993).
21. K. Takahei, A. Taguchi, and R. Hogg, "Atomic configurations of Er centers in GaAs: Er, O and AlGaAs: Er, O studied by site-selective luminescence spectroscopy," J. Appl. Phys. **82**(8), 3997–4005 (1997).
22. H. Ofuchi, T. Kubo, and M. Tabuchi, *et al.*, "Local structures around Er atoms in GaAs: Er, O studied by fluorescence EXAFS and photoluminescence," Microelectron. Eng. **51-52**, 715–721 (2000).
23. N. Chen, T. H. Xiao, and Z. Luo, *et al.*, "Porous carbon nanowire array for surface-enhanced Raman spectroscopy," Nat. Commun. **11**(1), 4772 (2020).
24. Y. Fujiwara, T. Kawamoto, and T. Koide, *et al.*, "Luminescence properties of Er, O-codoped III–V semiconductors grown by organometallic vapor phase epitaxy," Phys. B (Amsterdam, Neth.) **273-274**, 770–773 (1999).
25. K. Takahei, A. Taguchi, and Y. Horikoshi, *et al.*, "Atomic configuration of the Er-O luminescence center in Er-doped GaAs with oxygen codoping," J. Appl. Phys. **76**(7), 4332–4339 (1994).
26. G. S. Pomrenke, P. B. Klein, and D. W. Langer, *Rare earth doped semiconductors* (The Society, 1993).
27. A. Koizumi, Y. Fujiwara, and K. Inoue, *et al.*, "Room-temperature 1.54 μm light emission from Er, O-codoped GaAs/GaInP light-emitting diodes grown by low-pressure organometallic vapor phase epitaxy," Jpn. J. Appl. Phys. **42**(Part 1, No. 4B), 2223–2225 (2003).
28. A. Koizumi, Y. Fujiwara, and A. Urakami, *et al.*, "Room-temperature electroluminescence properties of Er, O-codoped GaAs injection-type light-emitting diodes grown by organometallic vapor phase epitaxy," Appl. Phys. Lett. **83**(22), 4521–4523 (2003).
29. A. M. Dibos, M. Raha, and C. M. Phenicie, *et al.*, "Atomic Source of Single Photons in the Telecom Band," Phys. Rev. Lett. **120**(24), 243601 (2018).
30. E. Miyazono, A. Hartz, and Z. Tian, *et al.*, "Hybrid quantum nanophotonic devices for coupling to rare-earth ions," in *2014 Conference on Lasers and Electro-Optics (CLEO) - Laser Science to Photonic Applications* (2014), pp. 1–2.

OPTICS CONTINUUM

31. T. Zhong, J. M. Kindem, and J. G. Bartholomew, *et al.*, "Optically addressing single rare-earth ions in a nanophotonic cavity," Phys. Rev. Lett. **121**(18), 183603 (2018).
32. S. Ritter, C. Nölleke, and C. Hahn, *et al.*, "An elementary quantum network of single atoms in optical cavities," Nature **484**(7393), 195–200 (2012).
33. D. Wang, H. Kelkar, and D. Martin-Cano, *et al.*, "Turning a molecule into a coherent two-level quantum system," Nat. Phys. **15**(5), 483–489 (2019).
34. D. Najer, I. Söllner, and P. Sekatski, *et al.*, "A gated quantum dot strongly coupled to an optical microcavity," Nature **575**(7784), 622–627 (2019).
35. R. Higashi, M. Ogawa, and J. Tatebayashi, *et al.*, "Enhancement of Er luminescence in microdisk resonators made of Er, O-codoped GaAs," J. Appl. Phys. **127**(23), 233101 (2020).
36. M. Ogawa, J. Tatebayashi, and N. Fujioka, *et al.*, "Quantitative evaluation of enhanced Er luminescence in GaAs-based two-dimensional photonic crystal nanocavities," Appl. Phys. Lett. **116**(18), 181102 (2020).
37. S. Ichikawa, Y. Sasaki, and T. Iwaya, *et al.*, "Enhanced red emission of Eu, O-codoped Ga N embedded in a photonic crystal nanocavity with hexagonal air holes," Phys. Rev. Appl. **15**(3), 034086 (2021).
38. D. Timmerman, Y. Matsude, and Y. Sasaki, *et al.*, "Purcell-Effect-Enhanced Radiative Rate of Eu $^{3+}$ Ions in Ga N Microdisks," Phys. Rev. Appl. **14**(6), 064059 (2020).
39. T. Iwaya, S. Ichikawa, and M. Murakami, *et al.*, "Design considerations of III-nitride-based two-dimensional photonic crystal cavities with crystallographically induced disorder," Appl. Phys. Express **14**(12), 122002 (2021).
40. T. Iwaya, S. Ichikawa, and D. Timmerman, *et al.*, "Improved Q-factors of III-nitride-based photonic crystal nanocavities by optical loss engineering," Opt. Express **30**(16), 28853–28864 (2022).
41. E. Kuramochi, H. Taniyama, and T. Tanabe, *et al.*, "Ultrahigh-Q one-dimensional photonic crystal nanocavities with modulated mode-gap barriers on SiO_2 claddings and on air claddings," Opt. Express **18**(15), 15859–15869 (2010).
42. M. Notomi, E. Kuramochi, and H. Taniyama, "Ultrahigh-Q nanocavity with 1D photonic gap," Opt. Express **16**(15), 11095–11102 (2008).
43. H. Tamura and H. Kurihara, "GaAs and GaAlAs reactive ion etching in BCl_3-Cl_2 mixture," Jpn. J. Appl. Phys. **23**(9A), L731 (1984).
44. M. Mochizuki, Y. Kitabayashi, and T. Nakajima, *et al.*, "dry etching of Al-rich AlGaAs for photonic crystal fabrication," Jpn. J. Appl. Phys. **50**(4S), 04DG15 (2011).
45. X. Zhang, K. Takeuchi, and X. Cong, *et al.*, "Dry etching of deep air holes in GaAs/AlGaAs-based epi-wafer having InAs quantum dots for fabrication of photonic crystal laser," Jpn. J. Appl. Phys. **56**(12), 126501 (2017).
46. A. Tandaechanurat, *Design of photonic crystals by FDTD method and fabrication of high-Q three-dimensional photonic crystal nanocavities*, (The University of Tokyo, 2009).